POST POINT WASTEWATER TREATMENT PLANT
Pipe Hanger Failure Investigation

Bellingham, Washington

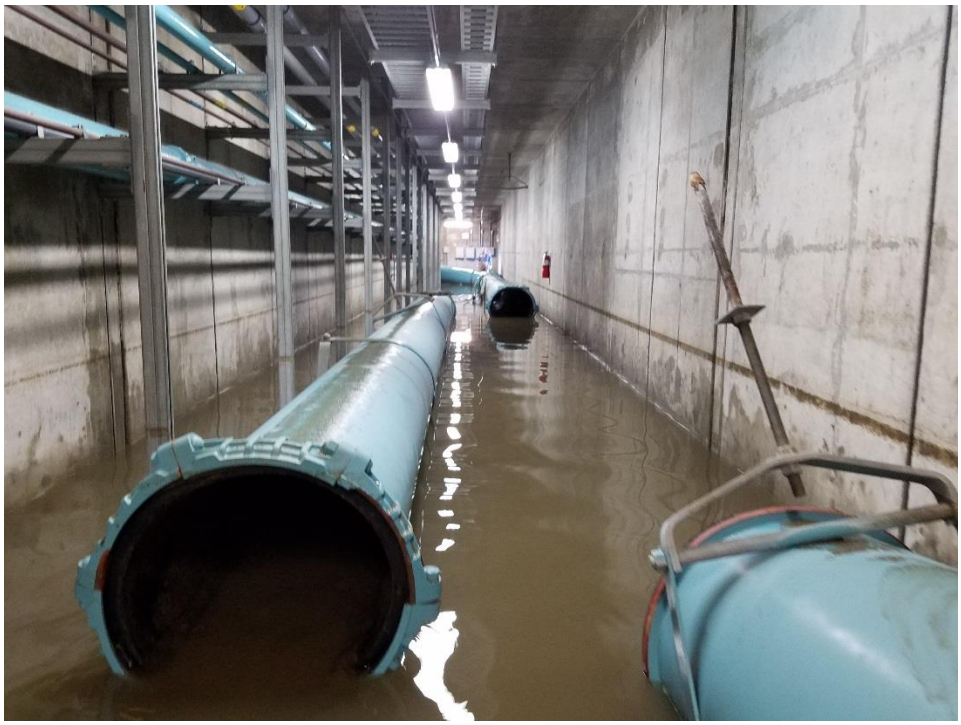

Report
December 7, 2017
WJE No. 2017.3338

Prepared for:
Carollo Engineers
1218 3rd Avenue, Suite1600
Seattle, Washington 98101

Prepared by:
Wiss, Janney, Elstner Associates, Inc.
960 South Harney Street
Seattle, Washington 98108
206.622.1441 tel | 206.622.0701 fax

POST POINT WASTEWATER TREATMENT PLANT
Pipe Hanger Failure Investigation

Bellingham, Washington

Zachary Stutts, P.E.
Associate III

Zeno Martin, P.E., S.E.
Project Manager

ZENO A. MARTIN
STATE OF WASHINGTON
38664
REGISTERED
PROFESSIONAL ENGINEER
12-7-2017

Report
December 7, 2017
WJE No. 2017.3338

Prepared for:
Carollo Engineers
1218 3rd Avenue, Suite 1600
Seattle, Washington 98101

Prepared by:
Wiss, Janney, Elstner Associates, Inc.
960 South Harney Street
Seattle, Washington 98108
206.622.1441 tel | 206.622.0701 fax

WJE ENGINEERS ARCHITECTS MATERIALS SCIENTISTS

TABLE OF CONTENTS

WJE ENGINEERS ARCHITECTS MATERIALS SCIENTISTS

POST POINT WASTEWATER TREATMENT PLANT
Pipe Hanger Failure Investigation

Bellingham, Washington

INTRODUCTION

At the request of Carollo Engineers, Wiss, Janney, Elstner Associates, Inc. (WJE) performed an investigation to determine the cause of failure of the structural hangers supporting a 30-inch diameter Return Activated Sludge (RAS) pipe at the Post Point Wastewater Treatment Plant (PPWWTP) located at 200 McKenzie Avenue in Bellingham, Washington. The RAS pipe is located in an interior corridor in a below grade structure at the plant and is suspended by pipe hangers for approximately 320 feet. Another 100 feet of the RAS pipe length is supported by bearing onto the interior corridor slab. The pipe hangers rely on threaded rods that extend above the RAS pipe that connect to the reinforced concrete lid of the corridor. On May 6, 2017, a number of threaded rod hangers that support the RAS pipe lost their connection to the concrete lid, causing collapse of the RAS pipe system and release of RAS into the interior corridor. Photos taken by Carollo shortly after the collapse indicated the threaded rods supporting the pipe experienced varying levels of corrosion. This report presents the findings of our investigation related to the cause of the failure of the pipe hanger system.

INVESTIGATION

WJE's investigation included the following:

- Meeting with Carollo Engineers Ms. Susanna Leung, P.E. and Mr. Tyler Whitehouse, P.E. to review project background.
- Document review. Various drawing sheets by CH2M Hill titled *City of Bellingham, Washington Post Point Wastewater Treatment Plan Upgrade*, dated August 1990.
- Site Observations. On August 31, 2017, Mr. Zeno Martin, P.E., S.E., and Mr. Zachary Stutts, P.E., of WJE visited the PPWWTP to observe and record conditions and collect material samples for subsequent laboratory analysis.
- Structural analysis to estimate demands imposed and capacity provided to resist the demands for the elements that were observed to be the primary cause of failure.
- Laboratory analysis to assess soil samples and the corroded steel components of seven hanger assemblies. Material samples were sent to WJE's Janney Technical Center in Northbrook, Illinois for analyses of soil characteristics, as well as the compositions of the steel components and their products of corrosion. The following samples from the site were sent in for laboratory analysis:
  - Soil Samples. Soil material samples were collected from four excavated soil locations termed potholes near where the soil was in contact with the concrete lid.
  - Threaded rods. The upper seven inches of the threaded rods labeled: Nos. 9 and 12, and B, C, E, G, and H.
  - Thread rod and nut assembly No. 19, extracted from Pothole No. 3 (this includes top nut, top washer, top plate, rod, bottom plate, bottom nut, and nut from on top of clevis).
  - Washer sample at failed rod assembly location No. 1 from Pothole No. 1.
  - Nut sample at failed rod assembly from Pothole No. 2.

FINDINGS

Background Information Related to Hanger Failure Provided to WJE

The structure that includes the below-grade corridor, along which the RAS pipe runs, was constructed as part of an early 1990s expansion of the PPWWTP.

The below-grade corridor runs between primary and secondary clarifiers and oxygen activated sludge basins. The construction of this corridor includes reinforced concrete walls, floor, and lid. Landscaping, including soil, plants, irrigation, and a maintenance road, occurs above the structure. As the RAS pipe exits the secondary sludge pump station, it is immediately supported by a series of pipe hangers (Figures 1 and 2). A total of twenty-eight pipe hangers support approximately 320 feet of pipe as shown in Appendix 1. The RAS pipe load remains generally constant, i.e., it is always nearly full of activated sludge, and the plant runs constantly.

Figure 1. Corridor with 30 inch diameter RAS Pipe (arrow) suspended from ceiling (lid). Photo provided to WJE by Carollo.

Figure 2. Typical pipe hanger. Photo provided to WJE by Carollo.

Some unspecified number of days or weeks prior to the May 6, 2017 collapse, it was reported by Carollo to WJE that PPWWTP staff had noticed that one of the RAS threaded galvanized steel pipe hangers, near Location 15 as shown in Appendix 1, had displaced vertically. WJE observed a photo taken by Carollo of this displaced hanger. The displacement appeared, by WJE's estimation, to be around an inch from its original position at the concrete ceiling. After observing this condition, PPWWTP staff installed temporary wood cribbing supports to the RAS pipe in the immediate vicinity of the displaced hanger to restore support to the RAS pipe at this location.

On May 6, 2017, a number of galvanized steel pipe hangers supported from the concrete lid of the below grade tunnel at the PPWWTP failed by pulling through the lid where they were connected, resulting in the collapse of a portion of the suspended steel RAS pipe (Figure 3). A total of thirteen pipe hangers lost their ability to remain connected to the concrete lid and pulled through it. Carollo reported to WJE that the collapsed segments of the RAS pipe had separated at the grooved end pipe joints, and the RAS pipe was slightly deformed to an oval shape from the vertical fall.

Figure 3. May 6, 2017 collapse of RAS pipe. Photo provided to WJE by Carollo.

Document Review

Design drawings dated August 1990 show pipe hanger construction detail for 18 to 30 inch diameter pipes (Figure 4), and for 4 to 16 inch diameter pipes (Figure 5). The size of the threaded hanger rod is not specified in Figure 5 beyond stating that it be "sized for load and spacing." The hanger rod is shown to be attached in a non-specific way to an element that is embedded into the concrete lid above. As described in the Site Observations section of this report, the as-constructed detail of the hanger rod to concrete lid connection differs from that shown in the original design drawings.

A section view detail of the concrete corridor specifies 18 inch thick concrete walls with two layers of reinforcement (each way inside face and outside face) and an 18 inch thick concrete lid with reinforcement in both directions on top and bottom. Bentonite waterproofing is specified all around the exterior of the concrete structure. The drawings do not specify or depict the pipe hangers to extend to the exterior of the concrete, as they were ultimately constructed, and so do not specify any waterproofing on the hanger components that extend to the exterior of the concrete. Drawings show the bottom of the suspended RAS pipe that is the subject of this report to be 8 feet above the concrete floor of the corridor, and show the corridor to be 12 feet wide and 12 feet tall.

The load path to support the suspended RAS pipe depicted in the original design drawings shows a transfer of the pipe load from a steel plate saddle and/or clevis to a rod "sized for load and spacing," and then to a hanger rod anchor or insert that is cast into the concrete lid above.

No shop drawings or other drawings depicting design or as-built conditions of the pipe hangers were available for WJE's review.

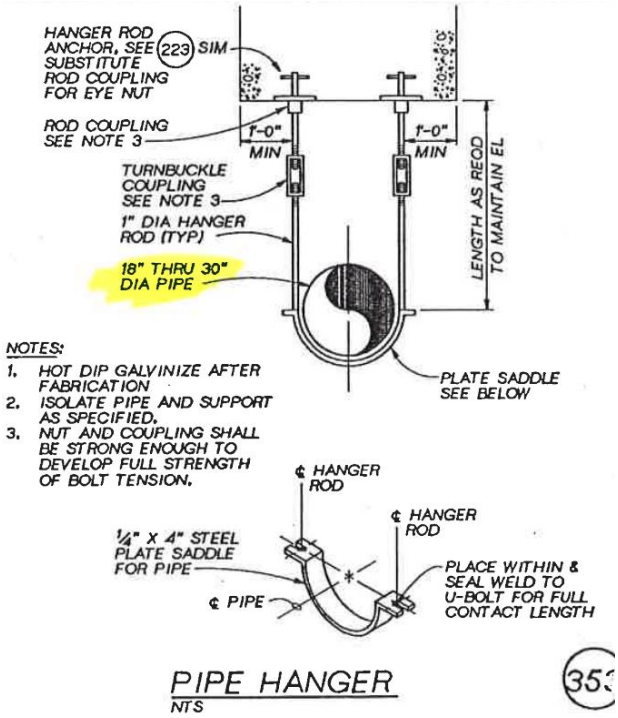

Figure 4. Pipe hanger specification from original design drawings for pipe diameters of 18 to 30 inches.

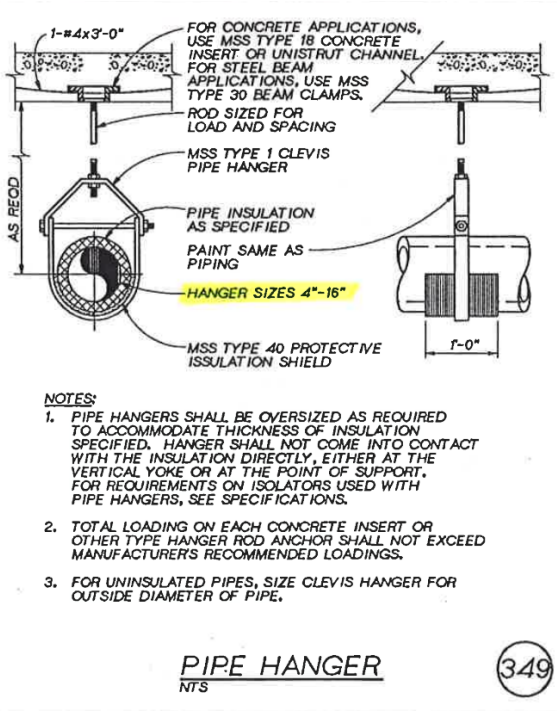

Figure 5. Pipe hanger specification from original design drawings for pipe diameters of 4 to 16 inches.

Site Observations

As-Constructed Hanger Rod to Concrete Lid Connection

The as-built RAS pipe hanger assembly and connection to the concrete lid do not match the design drawings from August 1990, and, instead, were attached to the concrete lid (Figure 6). As a result, the top of the threaded rod, nut, plate washer, and steel plate on top of the concrete lid were exposed to soil and moisture.

No apparent waterproofing or coatings beyond galvanizing appear to have been applied to the upper end of the threaded rod, nut, washer, and plate where they were in contact with soil. Grouting was not applied to fill the space between the threaded rod and the concrete, except a black material that appeared to be a sealant observed between the threaded rod and concrete surface (Figure 6).

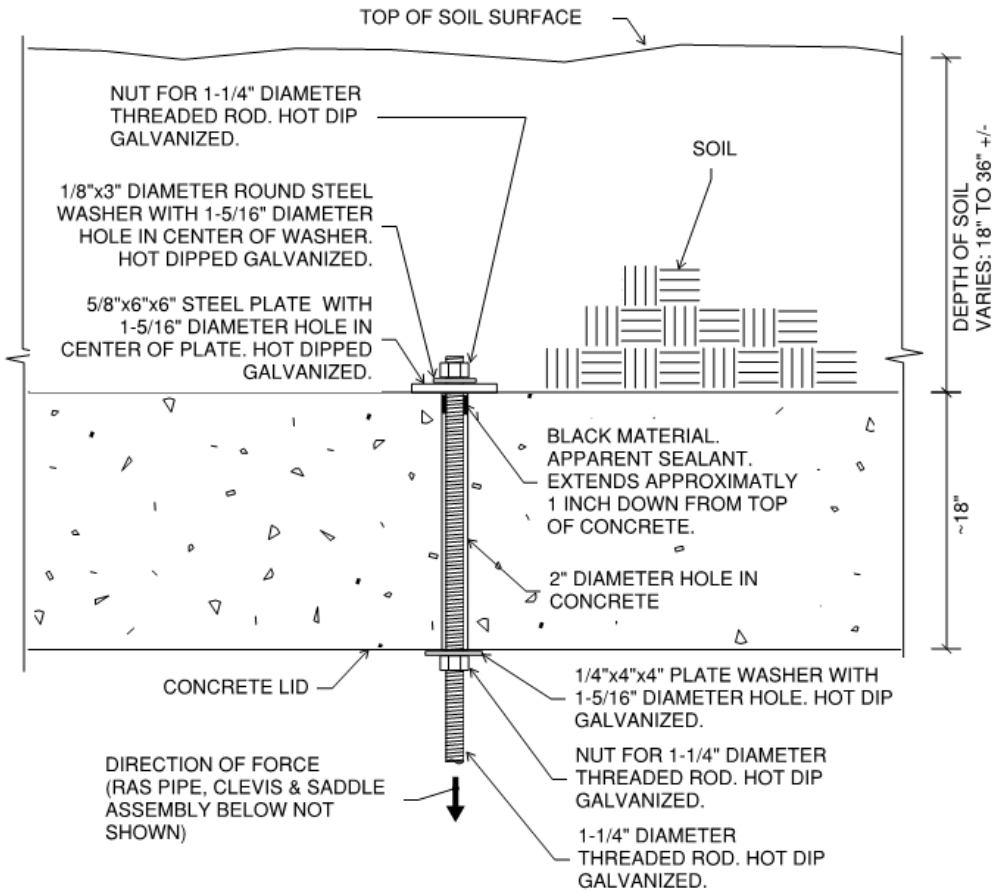

Figure 6. As-built section detail of threaded rod attachment to concrete lid.

The RAS pipe, clevis, and saddle assembly that were connected to the 1-1/4 inch diameter threaded rod are shown in Figures 1, 2, and 3. The clevis and saddle assembly connected to the 1-1/4 inch diameter threaded rod were similar to the clevis and saddle shown in Figure 5.

Storage Yard

Several weeks prior to WJE's August 31, 2017 site visit, PPWWTP staff and/or a contractor hired by PPWWTP had cleaned the corridor and removed the RAS pipe and the failed hanger elements (Figure 7).

Figure 7. Photo from a location of the corridor during WJE's site visit where the RAS pipe once was suspended but had been removed.

Hanger rods that had lost their connection to the concrete lid, along with associated attached components, were removed from the corridor and placed in a nearby storage yard on the site of the PPWWTP (Figure 8). Within the storage yard, WJE noted the presence of thirteen hanger rods, eight plate saddles, and eleven clevises. PPWWTP staff labeled some of the structural elements with their location in the corridor prior to their removal; other elements were found unlabeled. Five labeled threaded rods were uniquely found marked with 7, 9, 10, 11, and 12, which corresponded to numbers written on the wall in the corridor, which in turn correspond to locations shown in Appendix 1. The other threaded rods found unmarked were labeled onsite by WJE as A, B, C, D, E, F, G, and H.

All thirteen hanger rods located in the yard had failed by "pulling through" the concrete lid; other hanger rods that did not pull through the concrete lid remained in place in the corridor (Figure 9). The hanger rods that pulled through the concrete lid and were observed in the yard exhibited signs of severe corrosion on their upper tip that would have protruded above the concrete lid. An example of end of rod corrosion can be seen in Figures 10 and 11. A sketch indicating where the observed rod corrosion occurred in relation to its connection to the concrete lid is shown in Figure 12.

At Location 5, the steel pin component of the hanger assembly ruptured one side of the steel plate saddle to which it had been connected. All other saddles and clevises appeared to be intact without indication of physical damage.

Figure 8. Failed hanger rods were removed and placed in the PPWWTP storage yard.

Figure 9. Hanger rod that remains in place.

Figure 10. Corroded top of threaded rod. Rod labeled B by WJE.

Figure 11. Eroded top of threaded rod. Rod labeled E by WJE.

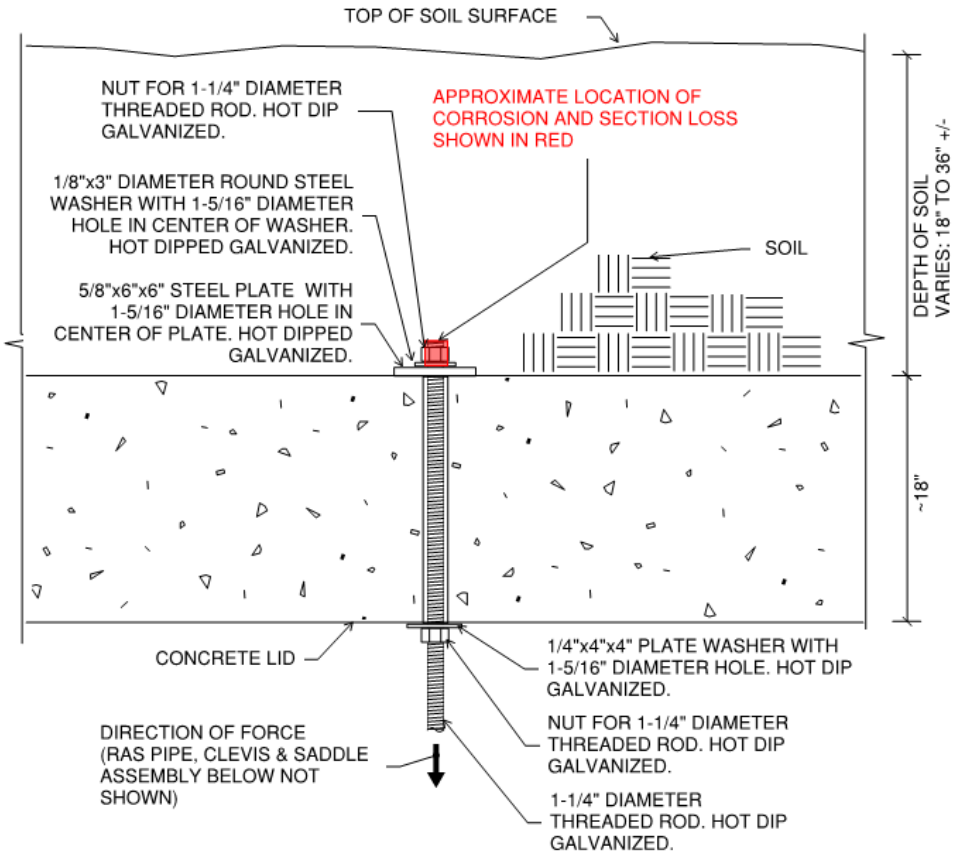

Figure 12. Depiction of approximate extent and location of corrosion and section loss (in red shaded region) observed at all rods that pulled through the lid.

Pothole Excavations

Prior to WJE's site visit, PPWWTP staff excavated soil by digging with hand shovels to expose four hanger connection conditions at the top of the concrete lid (Figures 13 and 14). The excavation was termed a pothole.

Figure 13. Pothole No. 2 with steel plate washer exposed. Round cut washer remnant of corroded nut removed by WJE prior to photo.

Figure 14. Pothole No. 3 shown with arrow, and WJE's Mr. Stutts standing in Pothole No. 4.

The soil and fill material placed above the concrete lid at the pothole excavations varied from about 18 inches in depth at Pothole Nos. 1 and 2 to approximately 36 inches at Pothole Nos. 3 and 4. Pothole Nos. 1 and 2 were above hanger rods that slipped (failed) through the lid, and Pothole Nos. 3 and 4 were above hanger rods that were still in place. See Appendix 1 for pothole locations.

At Pothole No. 1, the hanger rod that pulled through the concrete lid had been relocated to the holding yard with other samples. The plate washers were still in place. However, the nut that was holding the threaded rod was not found or observed, and the bottom of the pothole had water in it presumably from nearby landscape sprinklers (Figure 15).

At Pothole No. 2, the hanger rod that pulled through the concrete lid had been relocated to the holding yard with other samples. The plate washers were still in place, and the nut that was holding the threaded rod was found and observed to be corroded with nearly complete section loss. The nut was bagged and collected for laboratory examination (see Appendix 2 for photos of samples sent to the laboratory).

At Pothole Nos. 3 and 4, the entire plate assembly above the concrete lid was still intact, including the threaded hanger rod. Despite being intact, the components, and particularly the exposed nut, exhibited corrosion, including section loss of the nut (Figures 16 and 17). With the assistance of PPWWTP staff at Pothole No. 3, the hanger rod was cut from beneath the concrete lid, and WJE was able to extract the assembly for laboratory examination (Figure 18).

The concrete surface of the lid surrounding the plate washer appeared to be covered with a thin, approximately 1/4 inch thick layer of bentonite.

Figure 15. Pothole No. 1 with water at bottom and opening where threaded rod was once held by nut (arrow).

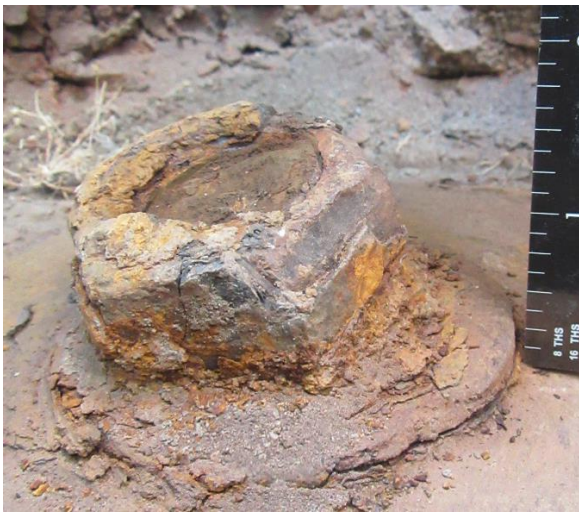

Figure 16. Pothole No. 3 steel washer and nut assembly in place. Note corrosion on nut and washer.

Figure 17. Pothole No. 4 steel washer and nut assembly in place. Note corrosion on nut.

Figure 18. Pothole No. 3 nut and washer rod assembly extracted for laboratory examination.

Bent Rods

Some threaded rods were observed to have a bend in them near the top of the concrete lid (Figure 19). Bends in the rods can also be seen in Figure 8 and the figures in Appendix 2. The unfailed sample extracted from Location 19 (at Pothole No. 3) also exhibited a bend in the rod, as shown in photographs of that sample in Appendix 2. The magnitude of the bends observed varied. During WJE's site visit, PPWWTP staff reported to WJE that during the original construction of the subject structure, after the concrete lid was constructed and after the threaded rods were installed, but before the concrete lid was covered with soil, they recalled that construction equipment had impacted the portions of the hanger components that extend above the concrete lid surface and hypothesized that the impact caused the bend. The impact described was implied to have imparted a lateral movement to the parts protruding above the concrete lid surface and thought to have maybe caused the bend in the rods.

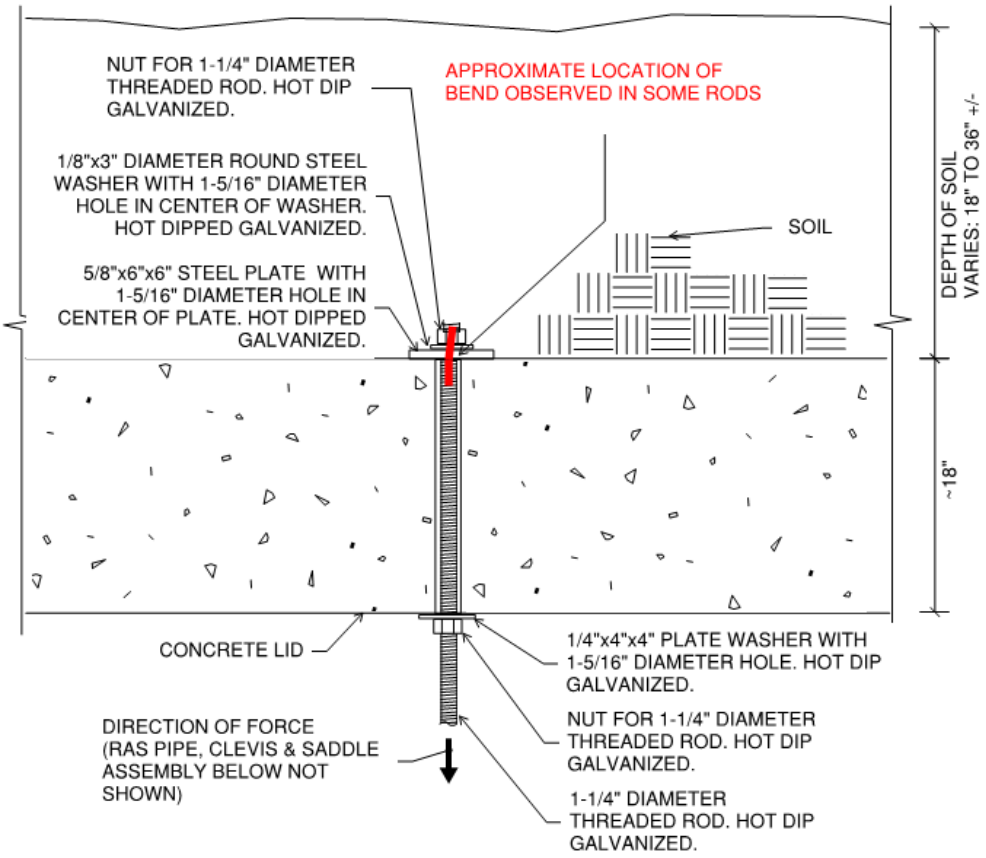

Figure 19. Depiction of approximate location of bend observed in some rods.

Structural Analysis

Structural analysis focus by WJE was limited to the components observed to be the primary cause of failure, which were the threaded rod, nut, and/or nut to rod threaded interface. The purpose of this analysis was to better understand and explain the failure mechanism observed. Quantitative structural analysis of components that did not exhibit observable evidence of distress, such as the 18 inch thick reinforced concrete lid, the clevis, or the RAS pipe, was not conducted.

While one support, at Location 5, had a fracture at the clevis saddle, no other locations exhibited the same. Such fracture is deemed by WJE to have followed the primary failure mode. The primary failure mode is evident to WJE by the fact that every threaded rod exhibited corrosion and section loss at its top. No other elements or components of the RAS pipe hanger assembly exhibited such a consistent pattern of distress as the corrosion and section loss at the tip of the threaded rod to nut interface. When the threaded rod to nut load transfer capacity was reduced due to corrosion to a level below that of the load imposed by the hanging RAS pipe, the threaded rod then failed to continue to perform as intended by losing its connection at the nut on top of the lid and pulled through the concrete lid, causing the RAS pipe to displace downward. The fracture at the clevis saddle at Location 5 occurred, in our opinion, because of the failures of the adjacent threaded rod supports due to the evidence of advanced corrosion at those locations.

As-Built Non-Corroded Conditions

The original construction of the RAS pipe structural support system is such that a pipe hanger assembly occurs approximately every 12 feet along the length of the pipe. This means that the load tributary to a hanger rod is also due to approximately 12 feet of pipe. The steel RAS pipe had a wall thickness of 1/4 inch, which means that a 30 inch diameter pipe would weigh 80 pounds per linear foot when empty. When the RAS pipe is full of activated sludge with the same density as water, the pipe's weight would increase to almost 380 pounds per linear foot. Based on these values, a single hanger rod then has about 4,500 pounds imposed on it in service.

A non-corroded 1-1/4 inch diameter rod (with 0.997 square inch gross area excluding threads), assuming it meets ASTM A36, the lowest of common thread rod standards and the assumed grade in use, would not be expected to rupture in tension until it has about 58,000 to 80,000 pounds on it.

The nut used on the threaded rod was measured by WJE and appears to meet the dimensions of an ASTM A563 hex nut. When these standard nuts and threads have full engagement along the length of the nut, the connection can develop, at a minimum, the tensile strength of the threaded rod. In the as-built assembly, the tension load from the hanging RAS pipe is transferred from the threads on the rod to the corresponding threads on the nut. The nut then bears onto the steel washer, which bears onto a steel plate, which bears onto the concrete lid. A diagram showing the load path between the threaded rod and nut is shown in Figure 20. When thread engagement between the nut and rod is only partial (Figure 21), the capacity is reduced proportionally per provisions of the Design Guide 1: *Base Plate and Anchor Rod Design* by the American Institute of Steel Construction. Therefore, an A563 hex nut on an ASTM A36 streel thread rod, with full engagement, would be expected to develop at least 58,000 to 80,000 pounds.

Analysis shows that the original non-corroded rod and nut to rod threaded engagement have about thirteen to eighteen times more ultimate tensile strength capacity than is imposed by the hanging RAS pipe.

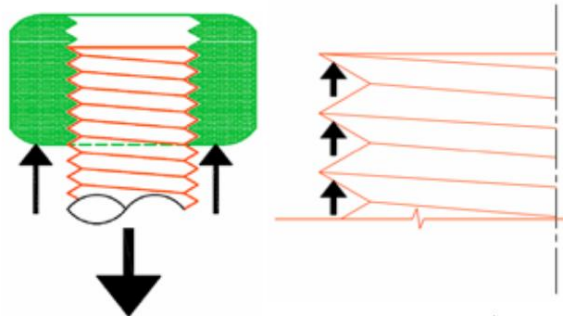

Figure 20. Load path depicted between threaded rod and nut.[1]

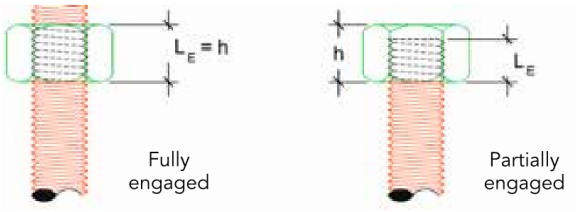

Figure 2. (Note: While protrusion through the nut is shown in the fully engaged example above, it is not necessary for full engagement.)

Figure 21. Depiction of full and partial nut to rod thread engagement.[1]

Effect of Corrosion on Capacity of Single Hanger

Corrosion that occurred caused loss of cross sectional area of the threaded rod, nut, and nut to rod interface. All thirteen failed rods observed in the storage yard, i.e., 100 percent of observed rods, exhibited corrosion and section loss at their tip where they were connected to a nut. In addition to the top of the rod corroding and diminishing in cross section (Figure 22), the nuts connected to the rod were also observed to have diminished cross section due to corrosion (Figure 23). All three nuts observed, i.e., 100 percent of observed nuts, including the nut recovered from Pothole No. 2 (Figure 21) and nuts from unfailed rods at Pothole Nos. 3 and 4, had corrosion and section loss (Figure 17 and 18).

Figure 22. Corroded top of threaded rod with loss of cross section from Rod Sample C.

Figure 23. Corroded nut once connected to threaded rod above the concrete lid from Location 2, Pothole No. 2.

[1] Image from Labelle, J., Strength and Engagement: Notes on Thread Strength and Partial Engagement of Anchor Rod Nuts, Modern Steel Construction, September 2016. https://www.aisc.org/globalassets/modern-steel/archives/2016/09/steelwise_2.pdf (accessed November 17, 2017).

As the nut and threads on the nut or on the rod lose steel due to the corrosion process, their capacity to transfer load is reduced due to the physical change. See a depiction of this mechanism in Figure 24.

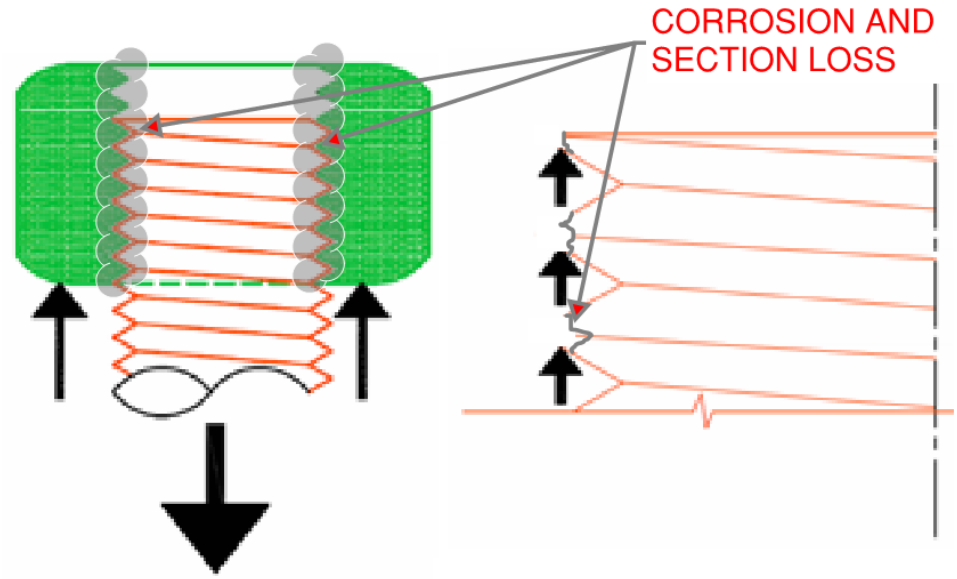

Figure 24. As corrosion and section loss occurs, the thread engagement between rod and nut is reduced, as is the capacity of the system to carry load. (Image modified from Figure 20).

The original non-corroded thread rod and nut would need to have about 92 to 95 percent reduction in material section in either the nut, rod, or threaded contact area interface before the assembly capacity would decrease sufficiently to no longer be expected to resist the imposed load of 4,500 pounds. Based on the observed section loss of the nut (Figure 23) and rods where they contacted the nut, section losses clearly exceeded 92 percent of the original in certain nuts and thread rod elements where they engaged each other.

Effect of Corrosion on Capacity of System

While corrosion and section loss were observed at the top of all hanger rods and nuts examined, the degree was not the same, i.e., some corroded more, some less. The RAS pipe itself, along with its connections, is relatively strong and stiff. Because the pipe is strong and stiff, it can span more than twelve feet and, thus, load can be distributed to adjacent hangers if one hanger fails, as demonstrated by the hanger slip (failure) prior to May 6, 2017. Failure of one hanger increases load imposed on adjacent hangers from 4,500 pounds to approximately 7,000 pounds (not including increased forces that may have been imparted due to the motion and impact resulting from downward displacement due to one hanger failing). One failed hanger assembly results in increased load on the pipe itself and adjacent hangers. If adjacent threaded rod and nut assembly portions of the hangers were not corroded sufficiently, they can certainly resist the added weight from one failed adjacent hanger since their original non-corroded capacity greatly exceeds weight imposed. However, that is not observed to be the case. The increased load was spread to adjacent hangers that were also affected by capacity reductions due to their corrosion and section loss, and so the failure spread in length along the RAS pipe span.

Laboratory Analysis

Samples

While on site, WJE collected the following samples from the site for laboratory analysis:

- Soil Samples. Soil material samples were collected from each of the four potholes near where the soil was in contact with the concrete lid.
- Threaded rods. The upper seven inches of the threaded rods labeled Nos. 9 and 12, and B, C, E, G, and H.
- Thread rod and nut assembly No. 19, extracted from Pothole No. 3 (this includes top nut, top washer, top plate, rod, bottom plate, and bottom nut).
- Washer sample at failed rod assembly location No. 1 from Pothole No. 1.
- Nut sample at failed rod assembly from Pothole No. 2.

Appendix 2 shows photos of all samples as received at the laboratory.

Material samples were sent to WJE's Janney Technical Center in Northbrook, Illinois for analyses of soil characteristics, as well as the compositions of the steel components and their products of corrosion. Also requested was a comparative assessment of the severity of the observed corrosion, given the service environment and timeframe involved.

Purpose of Testing

Laboratory analysis focused on the following:

- Soil samples were tested for the presence of salts or other chemicals to determine if there was a particularly corrosive environment present near the soil and threaded rod contact area.
- The threaded rod, nuts, and washers were tested to determine their material composition and to understand if dissimilar metals were present to assess the potential for galvanic corrosion.
- Corrosion products (rust) were tested to gain insight into what process was operating that could have accelerated the overall rate of corrosion observed.

A complete description of the laboratory testing conducted is contained in Appendix 3 of this report.

Results of Testing

Soil Samples. The results of electrical resistivity and pH of each soil sample are presented in Table 1.

Table 1. Soil Test Results

Sample	Hanger Condition	Resistivity (Ω•cm)	pH
Pothole No. 1	Failed	(not determined)	6.49
Pothole No. 2		2347	6.31
Pothole No. 3	Intact	4574	4.63
Pothole No. 4		2671	4.78

The electrical connectivity of the soil can be a major contributor to its corrosivity. Connectivity is the inverse of resistivity. So, a soil with low resistivity will have high connectivity. Salts (chlorides), for example, if present in the soil would be a contributor to lower the resistivity.

Soils with resistivity between 2,000 and 5,000 ohm-cm, which would include the soils analyzed here, are classified as "moderate to slight" in corrosivity.

Results do not indicate any outstanding characteristics to show that a particularly corrosive environment was created by elements of the soil.

Material Composition. The elemental compositions of three extensively corroded components taken from failed hanger assemblies, along with all of the components of intact Assembly No. 19 that had been retrieved from Pothole No. 3, were obtained by optical emission spectroscopy (OES). Steel is composed of iron and small amounts of other elements. The additional elements present in the structural components of interest are listed by weight percents in Tables 2 and 3. The limits specified by ASTM A36-2014, a specific standard of structural steel, are also given for reference purposes only, as the specific materials originally installed are not known.

Table 2. Compositions of Hanger Components from Failed Assemblies (Weight Percents)

Element	ASTM A36	Rod B	Washer No. 1	Top Nut No. 2
C	0.26 max	0.18	0.11	0.23
Mn	0.60–0.90	0.68	0.69	0.49
P	0.040 max	0.015	0.015	0.015
S	0.050 max	0.032	0.011	0.013
Si	0.40 max	0.22	0.18	0.20
Cr	(n/s)	0.15	0.05	<0.05
Ni	(n/s)	0.10	<0.05	<0.05
Mo	(n/s)	<0.05	<0.05	<0.05
Cu	(n/s)	0.32	<0.05	<0.05

Table 3. Compositions of Hanger Components from Intact Assembly No. 19 (Weight Percents)

Element	ASTM A36	Rod	Top Nut	Top Washer	Top Plate	Bottom Plate	Bottom Nut 1	Bottom Nut 2
C	0.26 max	0.19	0.21	0.07	0.20	0.15	0.20	0.20
Mn	0.60–0.90	0.83	0.49	0.38	0.47	0.74	0.47	0.49
P	0.040 max	0.028	0.014	0.016	0.008	0.014	0.016	0.014
S	0.050 max	0.038	0.012	0.016	0.012	0.028	0.014	0.012
Si	0.40 max	0.19	0.18	0.22	0.26	0.05	0.19	0.18
Cr	(n/s)	0.84	<0.05	<0.05	0.06	<0.05	<0.05	<0.05
Ni	(n/s)	0.14	<0.05	<0.05	0.08	<0.05	<0.05	<0.05
Mo	(n/s)	<0.05	<0.05	<0.05	<0.05	<0.05	<0.05	<0.05
Cu	(n/s)	0.10	<0.05	0.06	0.16	<0.05	<0.05	<0.05

Results show that the rod material could meet ASTM A36 based on its elemental composition. Results also show that differences in steel composition between different hanger components were not sufficient to have created an unusually strong galvanic cell at their interfaces. The potential for galvanic corrosion due to dissimilar metals between the threaded rod, nut, and washer is low and unlikely to have been a contributor to accelerating corrosion and section loss.

Corrosion Product. Corrosion product was removed from three samples for chemical analysis, which was carried out using scanning electron microscopy with energy dispersive x-ray spectroscopy (SEM/EDS), x-ray diffraction (XRD), and total sulfur measurements.

In the present case, SEM/EDS examination of the corrosion product samples indicated the presence of iron, oxygen, and carbon as the main components. The detected level of chlorine was generally minimal. The level of sulfur in the corrosion product was variable, with relatively low concentrations in the corrosion product of Rod B, and higher concentrations in the corrosion products of Rod E, and from both the nut and bolt of Rod 19. Sulfur, in the form of sulfate, can accelerate the corrosion of steel. The presence of sulfide corrosion products may indicate the activity of sulfate-reducing bacteria, which are known to accelerate corrosion of steel and may occur in soil environments.

XRD analysis detected the presence of goethite, lepidocrocite, and possibly detected nickelian pyrite and iron zinc. Goethite and lepidocrocite are common corrosion products of iron and steel. Nickelian pyrite and iron zinc are considered only possibly detected because each compound is only indicated by a single low-intensity peak rather than multiple peaks. Iron zinc may have been present because the materials were originally galvanized and would contain iron zinc intermetallic phases as part of the galvanized layer. The possible presence of nickelian pyrite may indicate the activity of sulfate-reducing bacteria in the corrosion process. To further evaluate the possibility of sulfide presence in the corrosion product, total sulfur contents were analyzed.

Total sulfur measurements of the corrosion product from the nut of Assembly No. 19 indicated 0.09 percent by mass of sample sulfide sulfur, and Rod H indicated 0.03 percent by mass of sample sulfide sulfur. While these values represent a small quantity overall of sulfide sulfur, they do indicate that a process to form sulfide in the corrosion product was present.

Laboratory Conclusions

1. The occurrence of more rapid corrosion at the interfaces between threaded rods and nuts at the top of the concrete lid was most likely due to crevice effects[2], specifically moisture maintenance and differential aeration.
2. Differences in steel component composition between failed and intact hangers were not sufficient to explain the observed variation in overall corrosion rate from one location to another.
3. Likely contributors to the more advanced degree of corrosion observed in some hanger locations as compared to others were average moisture level, degree of soil consolidation and aeration, and sulfide concentrations, possibly due to the concentrations and activity levels of sulfate-reducing bacteria.
4. Even accounting for the temporary protection afforded by galvanizing, the overall degree of metal loss exhibited by the components of failed hanger assemblies was consistent with their 25-year service exposure. Annual losses of 5 to 10 percent in saturated soil would not be unusual, particularly if crevice- and sulfate/sulfide-based mechanisms are active.

[2] Crevice corrosion occurs when moisture is present on the surfaces both inside and outside the interface between two components, at least one of which is metallic. In this case, the nut to threaded rod interface provides the surface to hold moisture. Initially the oxygen concentration in the water is equal throughout. However, as the oxygen inside the crevice reacts with the metal, its concentration in the water within the crevice falls below that of the water outside the crevice. This creates what is known as a differential aeration cell, in which the internal micro-environment causes the metal surface(s) within the crevice to become anodic relative to the adjacent external surfaces. The result is a significantly accelerated corrosion rate within the crevice.

CONCLUSION AND DISCUSSION

Mode of Failure

The suspended RAS pipe imposed a tension load onto the 1-1/4 inch diameter threaded rod connected to the pipe support elements. This tension load was resisted by a hex nut engaged with the rod. The hex nut bore onto a plate washer and steel plate that bore onto the top of the concrete lid. Analysis shows that the original non-corroded rod and nut to rod threaded engagement have about thirteen to eighteen times more ultimate tensile strength capacity than is imposed by the hanging RAS pipe, i.e., it had more than adequate structural capacity when it was originally installed. The top of the concrete lid, where the top of the threaded rod was engaged with the nut, was exposed to soil and moist conditions that created an environment conducive to corrosion.

Over time, corrosion occurred at the interface between the threaded rods and nuts at the top of the concrete lid, causing the failure to occur. This corrosion was due to the presence of moisture, crevice effects at the crevice between the threaded rod and nut and sulfate-reducing bacteria. The corrosion led to loss of original steel material of the threaded rod, nut, and their interfacing threads. As steel material was lost due to the corrosion process, the capacity for load transfer between the threaded rod to the nut was diminished. When the threaded rod to nut load transfer capacity was reduced to a level below that of the load imposed by the hanging RAS pipe, the threaded rod then failed by losing its connection at the nut on top of the lid and pulled through the concrete lid, causing the RAS pipe to displace downward.

Discussion of System Failure

The thirteen separate hanger rods that supported the RAS pipe and lost their ability to remain connected to the concrete lid all exhibited the same corrosion patterns at their interface between the threaded rods and nuts at the top of the concrete lid. Corrosion and section loss were also observed at the upper nut and portion of threaded rod in contact with soil in two hanger rod assemblies that had not failed (Pothole Nos. 3 and 4). The upper nut portions of threaded rods in contact with soil at other hanger rod locations that had not failed were not excavated for examination by WJE.

The probable sequence of the RAS pipe hanger system failure based on available information and logical plausibility is described as follows:

1. Corrosion and section loss occurred over twenty-five years (assuming parts were placed in service in 1992) at the interface between the threaded rods and nuts at the top of the concrete lid and advanced over time to the greatest extent at locations 1 through 4, 6 through 12, 15, and 24. Given the pattern that every location observed exhibited the same condition, we think it is likely that the other similar locations that were unobserved in our investigation also have corrosion and section loss to some degree.
2. As time progressed, section loss advanced.
3. When the RAS pipe hanger threaded rod to nut load transfer capacity was reduced due to corrosion to a level below that of the load imposed by the hanging RAS pipe, the threaded rod then failed by losing its connection at the nut on top of the lid and pulled through the concrete lid, causing the RAS pipe to displace downward.
4. The first reported failure occurred on an unspecified date prior to May 6, 2017. It was reported to WJE that PPWWTP staff had noticed that one of the RAS threaded pipe hangers, near Location 15, had displaced vertically, and was subsequently supported with temporary shores erected by PPWWTP staff.
5. On May 6, 2017, a location between 1 and 12 then experienced its threaded rod to nut load transfer capacity become reduced due to corrosion to a level below that of the load imposed by the hanging RAS pipe. The threaded rod then failed by losing its connection at the nut on top of the lid and pulled

through the concrete lid, causing the RAS pipe to displace downward. The loss of support at that one location then transferred load via the rigid RAS pipe to adjacent hanger locations. The adjacent hangers also had capacity reductions due to corrosion and section loss, and, with increased load imposed by the preceding failure of an adjacent hanger, they too failed. The system then "unzipped" until an equilibrium condition was found. The equilibrium condition was reached when the RAS pipe separated, rendering it unable to transfer additional load to other hangers and/or other hangers were not sufficiently affected by the same degree of corrosion related strength loss and, therefore, could still resist loads imposed on them.

Corrosion

The primary active corrosion mechanism appears to be crevice corrosion, with a sulfate/sulfide-based mechanism also evidently active.

Crevice corrosion occurs when moisture is present on the surfaces both inside and outside the interface between two components, at least one of which is metallic. In this case, the nut to threaded rod interface provides the surface to hold moisture. Initially the oxygen concentration in the water is equal throughout. However, as the oxygen inside the crevice reacts with the metal, its concentration in the water within the crevice falls below that of the water outside the crevice. This creates what is known as a differential aeration cell, in which the internal micro-environment causes the metal surface(s) within the crevice to become anodic relative to the adjacent external surfaces. The result is a significantly accelerated corrosion rate within the crevice, which is what was observed in this case.

Corrosion products analyzed found a process to form sulfide in the corrosion product was present. The presence of sulfide corrosion products indicates activity of sulfate-reducing bacteria, which are known to accelerate corrosion of steel.

As-Constructed vs. Specified Hanger Design

The original design drawings specified pipe hanger connections to the concrete lid to be embedded, or cast into place in the concrete lid. For steel cast into concrete, the high pH (alkalinity) of concrete provides the embedded steel with corrosion protection by formation of an oxide layer on the surface of the steel. The original specified design, which relied on embedded cast into place anchorage, would have been much less susceptible to corrosion than the as-built condition where the hot dipped galvanized steel hanger elements were directly exposed to moist soil. Whether or not the as-built RAS pipe hanger connection to the concrete lid was approved by the original design engineer, or by any others, is unknown to WJE.

APPENDIX 1

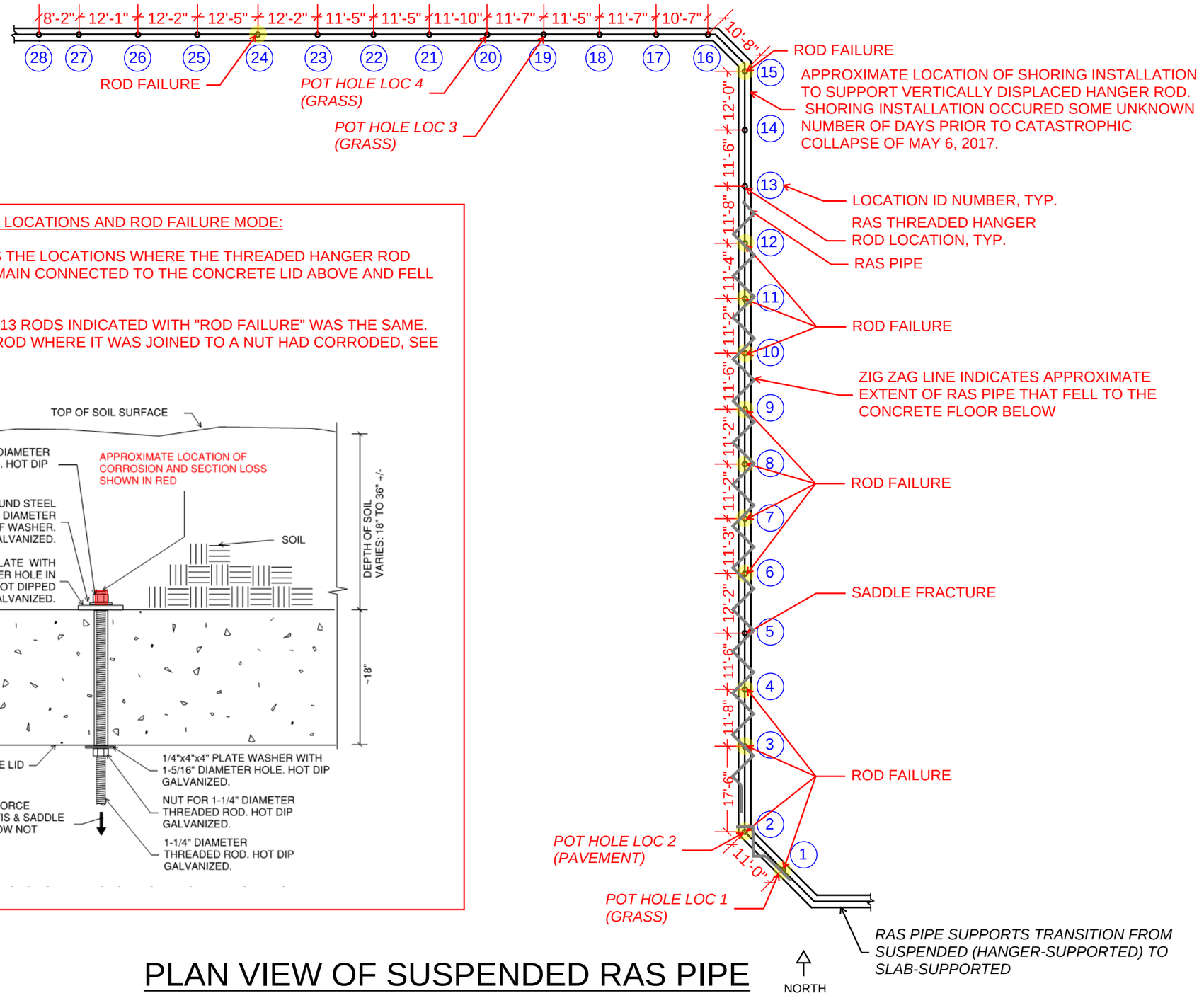

NOTES ON ROD FAILURE LOCATIONS AND ROD FAILURE MODE:

ROD FAILURE INDICATES THE LOCATIONS WHERE THE THREADED HANGER ROD LOST ITS ABILITY TO REMAIN CONNECTED TO THE CONCRETE LID ABOVE AND FELL DOWNWARD.

FAILURE MODE FOR ALL 13 RODS INDICATED WITH "ROD FAILURE" WAS THE SAME. THE UPPER TIP OF THE ROD WHERE IT WAS JOINED TO A NUT HAD CORRODED, SEE DETAIL 1 BELOW.

PLAN VIEW OF SUSPENDED RAS PIPE

WJE ENGINEERS ARCHITECTS MATERIALS SCIENTISTS

Wiss, Janney, Elstner Associates, Inc.
960 South Harney Street
Seattle, Washington 98108
206.622.1441 tel | 206.622.0701 fax
www.wje.com

Headquarters & Laboratories: Northbrook, Illinois
Atlanta | Austin | Boston | Chicago | Cleveland | Dallas | Denver | Detroit
Honolulu | Houston | Los Angeles | Minneapolis | New Haven | New York
Princeton | San Francisco | Seattle | Washington, D.C.

Seal

Consultant

Project

POST POINT WASTEWATER TREATMENT PLANT

Client

CAROLLO ENGINEERS

Mark	Date	Description

0 1/2" 1"

THIS SHEET PLOTS FULL SIZE AT 11x17 (INCHES)

Project No.	2017.3338
Date	8/31/2017
Drawn	ZS
Checked	ZM
Scale	NTS

PLAN VIEW OF SUSPENDED RAS PIPE

Sheet Title

SK-1

Sheet No.

APPENDIX 2

Cut end of rod for sample to be sent to lab

Corroded end of rod with section loss was tip in contact with soil.

Failed Rod 9_A

Cut end of rod for sample to be sent to lab

Corroded end of rod with section loss was tip in contact with soil.

Failed Rod 9_B

Commentary note: corroded end rod was tip in contact with soil.

Failed Rod 9_C

Commentary note: corroded end rod was tip in contact with soil.

Corroded end of rod with section loss was tip in contact with soil.

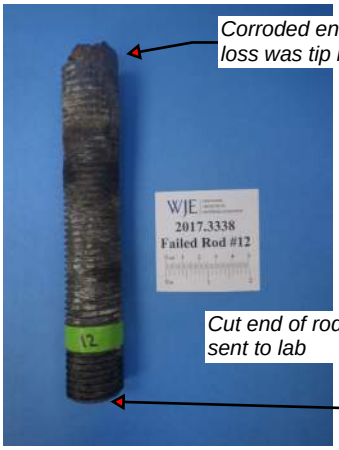

Cut end of rod for sample to be sent to lab

Failed Rod 12_A

Commentary note: corroded end rod was tip in contact with soil.

Corroded end of rod with section loss was tip in contact with soil.

Cut end of rod for sample to be sent to lab

Failed Rod 12_AA–corrected

Cut end of rod for sample to be sent to lab

Corroded end of rod with section loss was tip in contact with soil.

Failed Rod 12_B

Failed Rod 12_BB–corrected

Failed Rod 12_C

Corroded end of rod with section loss was tip in contact with soil.

Failed Rod 12_CC

Failed Rod 12_D

Corroded end of rod with section loss was tip in contact with soil.

Failed Rod 12_DD

Failed Rod 12_EE

Corroded end of rod with section loss was tip in contact with soil.

Failed Rod B_A

Failed Rod B_B

Failed Rod B_C

Corroded end of rod with section loss was tip in contact with soil.

Failed Rod C_A

Failed Rod C_B

Corroded end of rod with section loss was tip in contact with soil.

Failed Rod C_C

Failed Rod C_D

Failed Rod C_E

Corroded end of rod with section loss was tip in contact with soil.

Failed Rod E_A

Failed Rod E_B

Failed Rod E_C

Failed Rod E_D

Corroded end of rod with section loss was tip in contact with soil.

Failed Rod E_E

Failed Rod E_F

Corroded end of rod with section loss was tip in contact with soil.

Failed Rod E_G

Failed Rod E_H

Corroded end of rod with section loss was tip in contact with soil.

Failed Rod G_A

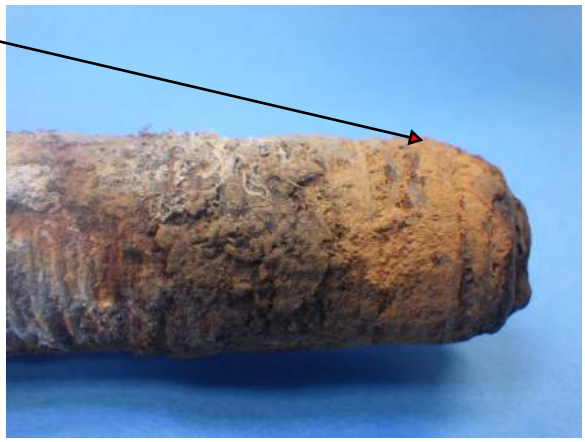

Failed Rod G_B

Failed Rod G_C

Failed Rod G_D

Corroded end of rod with section loss was tip in contact with soil.

Failed Rod G_E

Failed Rod G_F

Failed Rod G_G

Corroded end of rod with section loss was tip in contact with soil.

Failed Rod H_A

Failed Rod H_B

Failed Rod H_C

Corroded end of rod with section loss was tip in contact with soil.

Failed Rod H_D

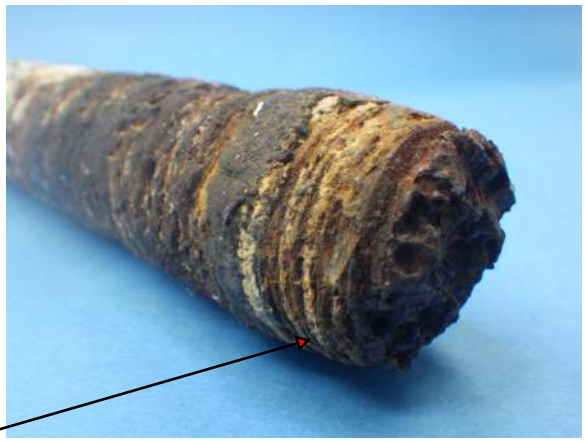

Failed Rod H_E

Corroded end of rod with section loss was tip in contact with soil.

Corroded end of rod with section loss was tip in contact with soil.

Non-failed Rod Assembly 19

Non-failed Rod Assembly 19

Corroded end of rod with section loss was tip in contact with soil.

Non-failed Rod Assembly 19

Non-failed Rod Assembly 19

Non-failed Rod Assembly 19

Non-failed Rod Assembly 19

Non-failed Rod Assembly 19

Non-failed Rod Assembly 19

Non-failed Rod Assembly 19

Corroded end of rod with section loss was tip in contact with soil.

Non-failed Rod Assembly 19

Corroded end of rod with section loss was tip in contact with soil.

Non-failed Rod Assembly 19

Nut Sample Failed Rod Assembly

Nut Sample Failed Rod Assembly

Nut Sample Failed Rod Assembly

Nut Sample Failed Rod Assembly

Nut Sample Failed Rod Assembly

Nut Sample Failed Rod Assembly

Nut Sample Failed Rod Assembly

Nut Sample Failed Rod Assembly

Nut Sample Failed Rod Assembly

Soil Sample Pothole 1_A

Soil Sample Pothole 1_B

Soil Sample Pothole 1_C

Soil Sample Pothole 1_D

Soil Sample Pothole 2_A

Soil Sample Pothole 2_B

Soil Sample Pothole 2_C

Soil Sample Pothole 3_A

Soil Sample Pothole 3_B

Soil Sample Pothole 3_C

Soil Sample Pothole 4_A

Soil Sample Pothole 4_B

Soil Sample Pothole 4_C

Washer Sample Failed Rod Assembly 1

Washer Sample Failed Rod Assembly 1

Washer Sample Failed Rod Assembly 1

Washer Sample Failed Rod Assembly 1

APPENDIX 3

WJE ENGINEERS ARCHITECTS MATERIALS SCIENTISTS

Wiss, Janney, Elstner Associates, Inc.
330 Pfingsten Road
Northbrook, Illinois 60062
847.272.7400 tel | 847.291.5189 fax
www.wje.com

INTEROFFICE MEMORANDUM

To: Zeno Martin

From: Robert Warke, Kimberly Steiner and Jeff Plumridge

Date: October 27, 2017

Project: PPWWTP RAS Pipe Hanger Failure Investigation
WJE No. 2017.3338

Subject: Laboratory Analyses of Soil, Steel and Corrosion Product Samples

---

Soil samples from four potholes and the corroded steel components of seven hanger assemblies were submitted to WJE's Janney Technical Center in Northbrook, Illinois for analyses of soil characteristics, as well as the compositions of the steel components and their products of corrosion. Also requested was a comparative assessment of the severity of the observed corrosion, given the service environment and timeframe involved.

Testing of Soil

Measurements of the electrical resistivity and pH of each soil sample were undertaken. Resistivity was measured essentially in accordance with ASTM G187 *Standard Test Method for Measurement of Soil Resistivity Using the Two-Electrode Soil Box Method*. Prior to resistivity testing, the soil sample was saturated with deionized water. Insufficient sample volumes were received to completely fill the soil box; therefore, the height of the soil in the box was incorporated into each resistivity calculation. The very small volume of soil from Pothole #1 precluded resistivity measurement altogether. The pH of each saturated soil sample was measured using an Extech meter with a flat surface electrode. The results of both tests are presented in Table 1.

Table 1. Soil Test Results

Sample	Hanger Condition	Resistivity (Ω•cm)	pH
Pothole #1	Failed	(not determined)	6.49
Pothole #2		2347	6.31
Pothole #3	Intact	4574	4.63
Pothole #4		2671	4.78

Analysis of Steel Composition

The elemental compositions of three extensively corroded components taken from failed hanger assemblies, along with all of the components of intact Assembly #19 that had been retrieved from Pothole 3, were obtained by optical emission spectroscopy (OES). The results are listed in Tables 2 and 3. The limits specified by ASTM A36–2014 are also given, for reference purposes only, as the compositions originally specified were not available.

Table 2. Compositions of Hanger Components from Failed Assemblies (Weight Percents)

Element	ASTM A36	Rod B	Washer #1	Top Nut #2
C	0.26 max	0.18	0.11	0.23
Mn	0.60–0.90	0.68	0.69	0.49
P	0.040 max	0.015	0.015	0.015
S	0.050 max	0.032	0.011	0.013
Si	0.40 max	0.22	0.18	0.20
Cr	(n/s)	0.15	0.05	<0.05
Ni	(n/s)	0.10	<0.05	<0.05
Mo	(n/s)	<0.05	<0.05	<0.05
Cu	(n/s)	0.32	<0.05	<0.05

Table 3. Compositions of Hanger Components from Intact Assembly #19 (Weight Percents)

Element	ASTM A36	Rod	Top Nut	Top Washer	Top Plate	Bottom Plate	Bottom Nut 1	Bottom Nut 2
C	0.26 max	0.19	0.21	0.07	0.20	0.15	0.20	0.20
Mn	0.60–0.90	0.83	0.49	0.38	0.47	0.74	0.47	0.49
P	0.040 max	0.028	0.014	0.016	0.008	0.014	0.016	0.014
S	0.050 max	0.038	0.012	0.016	0.012	0.028	0.014	0.012
Si	0.40 max	0.19	0.18	0.22	0.26	0.05	0.19	0.18
Cr	(n/s)	0.84	<0.05	<0.05	0.06	<0.05	<0.05	<0.05
Ni	(n/s)	0.14	<0.05	<0.05	0.08	<0.05	<0.05	<0.05
Mo	(n/s)	<0.05	<0.05	<0.05	<0.05	<0.05	<0.05	<0.05
Cu	(n/s)	0.10	<0.05	0.06	0.16	<0.05	<0.05	<0.05

Analysis of Corrosion Product

Corrosion product was removed from three samples for chemical analysis, which was carried out using scanning electron microscopy with energy dispersive x-ray spectroscopy (SEM/EDS), x-ray diffraction (XRD), and total sulfur measurements.

SEM/EDS

Samples from the failed rods identified as Rod B and Rod E, and the nut from non-failed Assembly #19, were analyzed using SEM/EDS. Figure 1– contain photographs showing locations where corrosion product was removed for analysis.

In SEM, a beam of electrons is generated, focused, and scanned across a very small area of the sample. The electrons interact with the sample in various ways that can be exploited to image and characterize the material. Two electron-based imaging modes are possible: backscattered and secondary. In backscattered electron (BE) imaging, electrons from the incident beam that have been backscattered or elastically reflected by the elements in the sample are collected by a BE detector. Heavier atoms in the sample scatter the beam electrons to a greater degree than lighter atoms, causing phases with a higher average atomic weight to appear brighter in the resulting image than phases with a lower average atomic weight. This provides compositional information within the image. Secondary electron (SE) imaging makes use of

electrons that are emitted from the sample as a result of inelastic interactions with the beam, which provides information related to its surface topography.

The interaction of beam electrons with the sample also generates characteristic x-rays. The energies of the characteristic x-rays can be measured using EDS, producing an energy peak spectrum that enables identification of elements present in the sample. EDS data can be collected from a single point volume of material a few microns wide, or from a scan over a selected area. Prior to analysis by SEM/EDS, a corrosion product sample is typically coated with a thin layer of conductive carbon to minimize the buildup of electrical charge. This carbon appears in the EDS spectrum; therefore, for some samples, it cannot be determined whether the carbon is from the sample itself or the carbon coating. Because EDS is an elemental spectroscopy technique, elements present can be detected, but the manner in which the elements are combined to form compounds is not provided directly. However, compounds present can often be inferred on the basis of elemental ratios and prior experience.

In the present case, SEM/EDS examination of the corrosion product samples indicated the presence of iron, oxygen, and carbon as the main components. Varying amounts of other elements, including silicon, magnesium, zinc, sulfur, phosphorus, calcium, aluminum, magnesium, chlorine, chromium, manganese, nickel, and copper were also detected. Some of these elements had been incorporated into the corrosion product from the surrounding soil. The detected level of chlorine was generally minimal. The level of sulfur in the corrosion product was variable, with relatively low concentrations in the corrosion product of Rod B (Figure 4 and Figure 5), and higher concentrations in the corrosion product of Rod E (Figure 6 and Figure 7) and the corrosion product from both the nut and bolt of Rod 19 (Figures 8 through 10). Sulfur, in the form of sulfate or sulfide, can accelerate the corrosion of steel. For example, the presence of sulfide corrosion products may indicate the activity of sulfate-reducing bacteria, which are known to accelerate corrosion of steel, and may occur in soil environments. Since EDS is an elemental spectroscopy technique, the data only indicates the presence of the element sulfur, and does not indicate whether it is present as sulfate (SO_4^{2-}) or sulfide (S^{2-}). For that reason, other analyses were performed.

XRD

X-ray diffraction (XRD) analysis is suitable for identifying crystalline compounds. During XRD analysis, incident radiation from an x-ray source is diffracted from the sample at various angles whose values depend on the characteristic geometry of the crystal structures that are present. A detector measures the intensity of the diffracted energy for each angle, and the location (angle) and intensity are recorded as a graph containing a pattern of peaks. The peaks are compared to a library of diffraction patterns of known components, which enables interpretation of the graph to identify the crystalline components of the sample.

Corrosion products are typically mixtures of different phases, with some portion of the mixture frequently poorly crystalline or non-crystalline. However, XRD analysis can provide some information on how the components are combined to form crystalline compounds. For this reason, and, in particular, to evaluate the potential sulfur-containing compounds, a sample from the nut of Assembly #19 was analyzed using XRD.

XRD analysis detected the presence of goethite (FeOOH), lepidocrocite (FeOOH), and possibly detected nickelian pyrite [$(Fe,Ni)S_2$] and iron zinc ($FeZn_{6.67}$). Goethite and lepidocrocite are common corrosion products of iron and steel. Nickelian pyrite and iron zinc are considered only possibly detected because each compound is only indicated by a single low-intensity peak rather than multiple peaks. Iron zinc may

have been present because the materials were originally galvanized, and would contain iron zinc intermetallic phases as part of the galvanized layer. The possible presence of nickelian pyrite may indicate the activity of sulfate-reducing bacteria in the corrosion process. To further evaluate the possibility of sulfide presence in the corrosion product, total sulfur contents were analyzed.

Total Sulfur Content

The concentration of sulfide compared to sulfate in the corrosion product was measured essentially according to the methodology outlined in ASTM E1915 *Standard Test Methods for Analysis of Metal Bearing Ores and Related Materials for Carbon, Sulfur, and Acid-Base Characteristics.* Total sulfur measurements were made on as-received samples and samples after heating to 550°C for one hour, which eliminates the sulfate. The difference between these two values is the sulfide sulfur. Corrosion product from the nut of Assembly #19 and the end of Rod H were tested. Rod H was selected based on its similarity to Rod B and the quantity of material available for testing. Insufficient material from Rod E was available for testing. Based on this analysis, corrosion product from the nut of Assembly #19 indicated 0.09 percent by mass of sample sulfide sulfur, and Rod H indicated 0.03 percent by mass of sample sulfide sulfur. While these values represent a small quantity overall of sulfide sulfur, they do indicate that a process to form sulfide in the corrosion product was present.

Discussion

Corrosion of steel in soil is a complex process and the specific conditions that lead to accelerated corrosion rates are not well characterized, and the performance of steel in-ground is not as well understood as in above-ground applications. Many studies of corrosion of buried pipe and other metallic materials have been conducted to evaluate soil characteristics and their effect on corrosion (Chaker and Palmer 1989, Cole and Marney 2012, Wilmot and Jack 2000). While the effect of a given parameter cannot be used to provide conclusive identification of a given soil as corrosive or non-corrosive, some trends are apparent. Generally, important characteristics for soil include degree of disturbance, moisture content, pH, resistivity, oxidation/reduction potential, and sulfide content.

Disturbed soils, including soils that have been excavated and backfilled over the component of interest, are associated with a greater degree of corrosion as compared to undisturbed soils, including metallic components that have been pile-driven. Relatively dry soils are associated with lower corrosion rates than moist to wet soils. On the other hand, soils below the water table may be associated with lower corrosion rates than similar soils above the water table, due to lower concentrations of oxygen and corrosive species. Soils that are acidic are generally associated with a greater corrosivity than alkaline soils. Soils with higher electrical resistivity are both more resistant to current flow and have a lower ionic concentration, therefore are associated with lower corrosion rates than less resistive soils. Soils with a low oxidation/reduction potential (anoxic soils) may harbor anaerobic (sulfate-reducing) bacteria and have a higher corrosion rate than oxidizing soils. Sulfide content can be an indicator of sulfate-reducing bacteria, as well as a low oxidation/reduction potential. Because oxidation/reduction potential and sulfide concentration are liable to change upon soil being disturbed and exposed to greater quantities of oxygen, these parameters must be measured in-situ, rather than in the laboratory after the samples were collected.

The American Water Works Association has developed a rating system for corrosion of ductile iron pipe in soils, as given in AWWA C105 *American National Standard for Polyethylene Encasement for Ductile-Iron Pipe Systems*. AWWA C105 assigns points for various parameters, with the total number of points

indicating whether polyethylene encasement is required to protect the pipe from the soil environment. Based on the resistivities and pH values measured, the soils analyzed in the present case would not indicate the need for protection of ductile iron, assuming the absence of other factors that contribute to corrosivity. Another source classifies soils for their corrosivity to steel, which is generally more susceptible than ductile iron to corrosion in soils. In this system, soils with resistivities between 2,000 and 5,000 ohm-cm, which would include the soils analyzed here, are classified as "moderate to slight" in corrosivity.

Conclusions

1. Comparisons of soil samples taken from failed and intact hanger locations were inconclusive in terms of electrical resistivity, and actually opposite the expected trend in terms of acidity.
2. Differences in steel composition between different hanger components were not sufficient to have created an unusually strong galvanic cell at their interfaces.
3. The occurrence of more rapid corrosion at the interfaces between hanger assembly components was most likely due to crevice effects, by moisture maintenance through capillary action and the formation of differential aeration cells.
4. Differences in steel component composition between failed and intact hangers were not sufficient to explain the observed variation in overall corrosion rate from one location to another.
5. Likely contributors to the more advanced degree of corrosion observed in some hanger locations as compared to others were average moisture level, degree of consolidation and aeration, and sulfide concentrations, possibly due to the concentrations and activity levels of sulfate-reducing bacteria.
6. Even accounting for the temporary protection afforded by galvanizing, the overall degree of metal loss exhibited by the components of failed hanger assemblies was consistent with their 25-year service exposure. Annual losses of 5–10% in saturated soil would not be unusual, particularly if crevice- and sulfate/sulfide-based mechanisms are active.

References

Chaker, V. and Palmer, J. D., Eds. 1989. ASTM Committee G-1 on Corrosion of Metals. Effects of Soil Characteristics on Corrosion. Philadelphia: ASTM.

Cole, I. S., and Marney, D. 2012. "The science of pipe corrosion: A review of the literature on the corrosion of ferrous metals in soils." Corrosion Science 5-16.

Wilmot, M. J., and T. R. Jack. 2000. "Corrosion by Soils." In Uhlig's Corrosion Handbook, by R. Winston, Editor Revie. New York: John Wiley & Sons, Inc.

Figures

Figure 1. Corrosion product was collected from the indicated area of Sample Rod B for SEM/EDS analysis.

Figure 2. Corrosion product was collected from the indicated area of Rod E for SEM/EDS analysis.

Figure 3. Corrosion product was collected from the indicated area of Assembly #19 for SEM/EDS analysis.

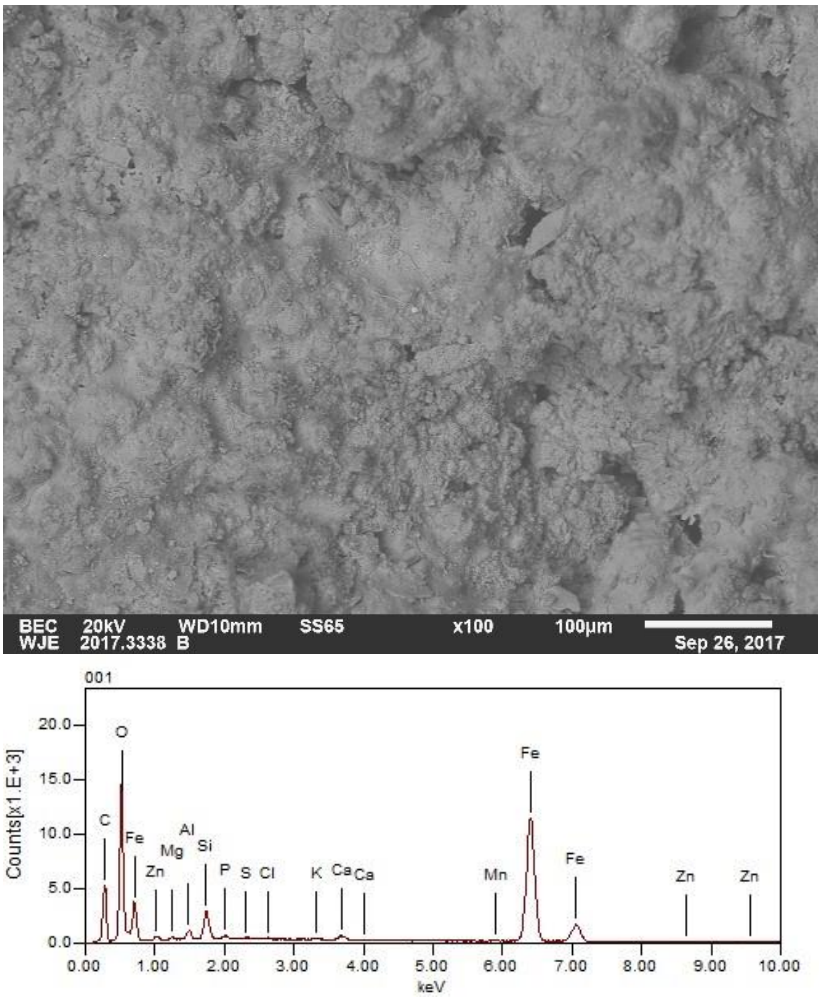

Figure 4. BE micrograph and area EDS spectrum of corrosion product removed from Rod B.

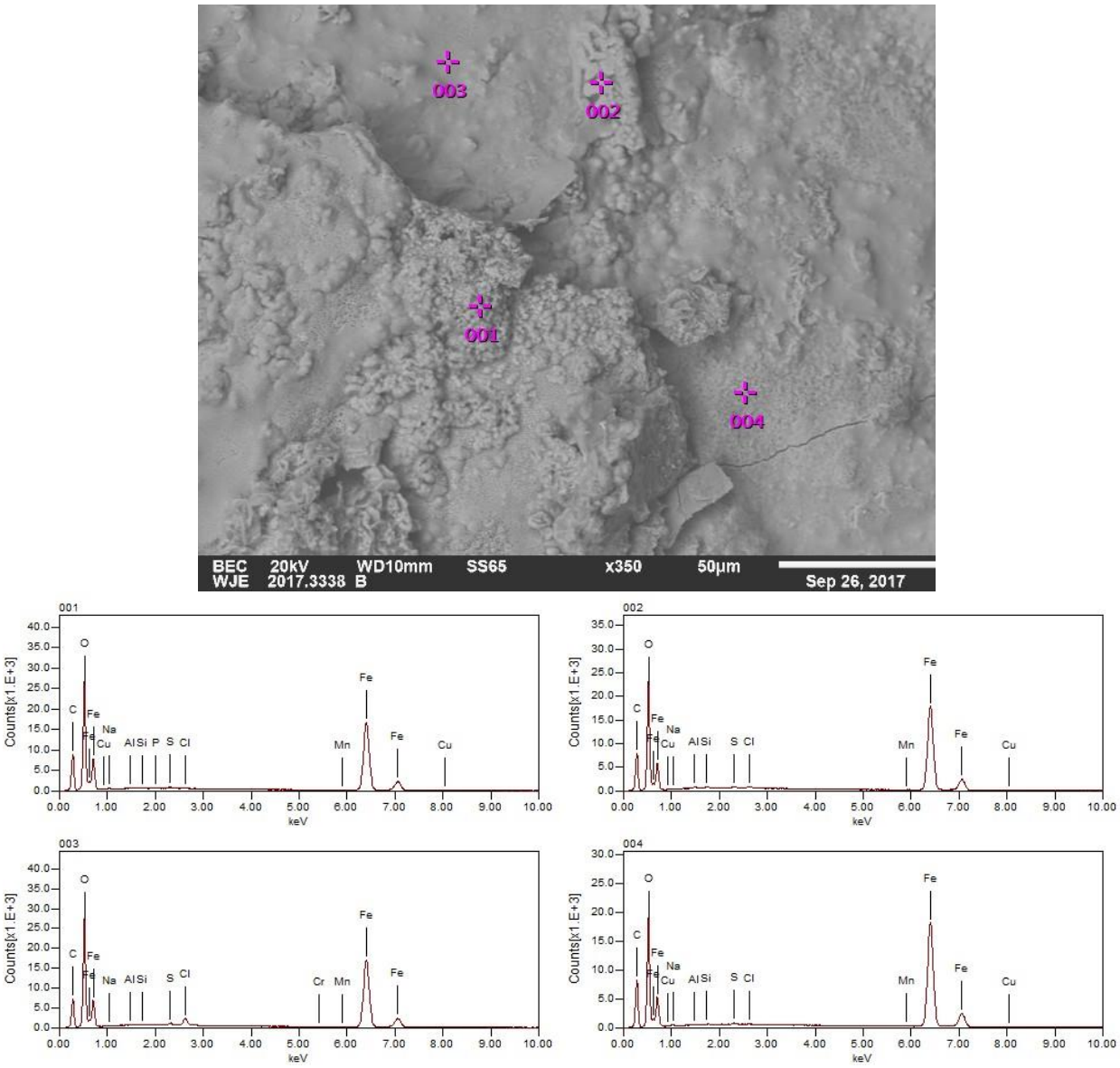

Figure 5. BE micrograph and EDS point spectra of corrosion product removed from Rod B. Each EDS spectrum has a number in the upper left corner that corresponds to a point with the same designation in the micrograph.

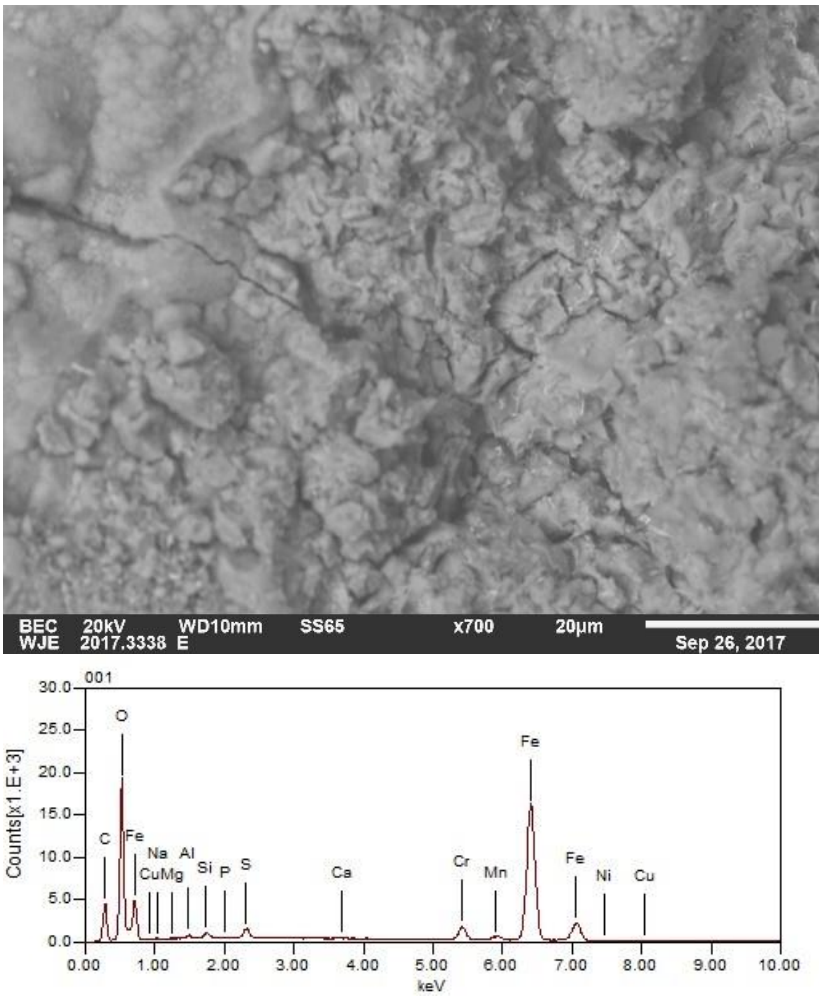

Figure 6. BE micrograph and area EDS spectrum of corrosion product removed from Rod E.

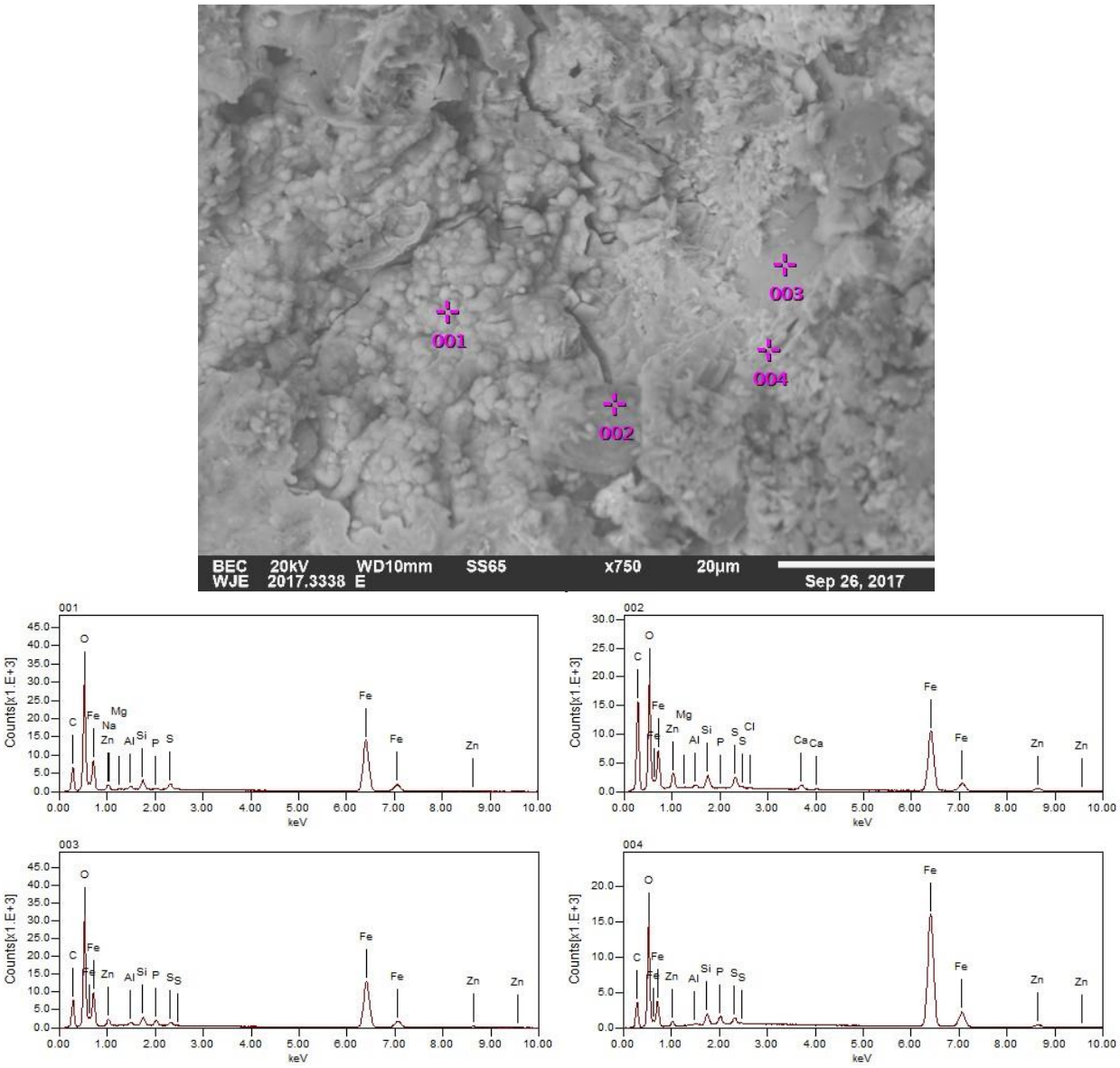

Figure 7. BE micrograph and EDS point spectra of corrosion product removed from Rod E. Each EDS spectrum has a number in the upper left corner that corresponds to a point with the same designation in the micrograph.

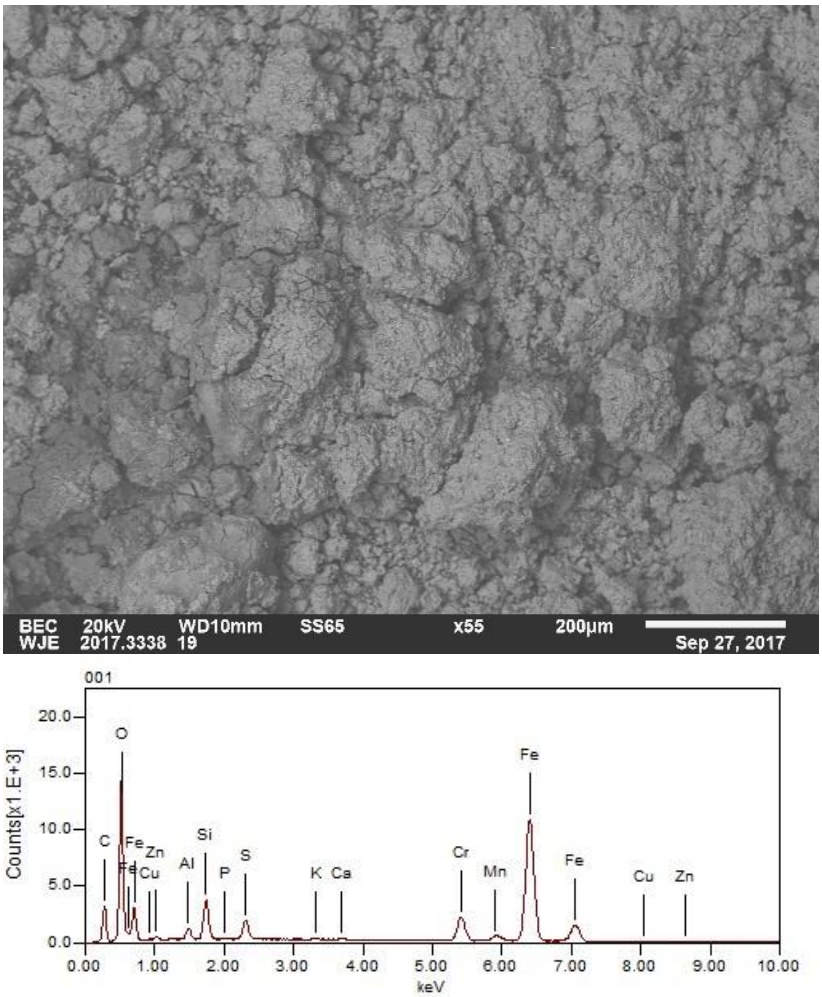

Figure 8. BE micrograph and area EDS spectrum of corrosion product removed from Assembly #19.

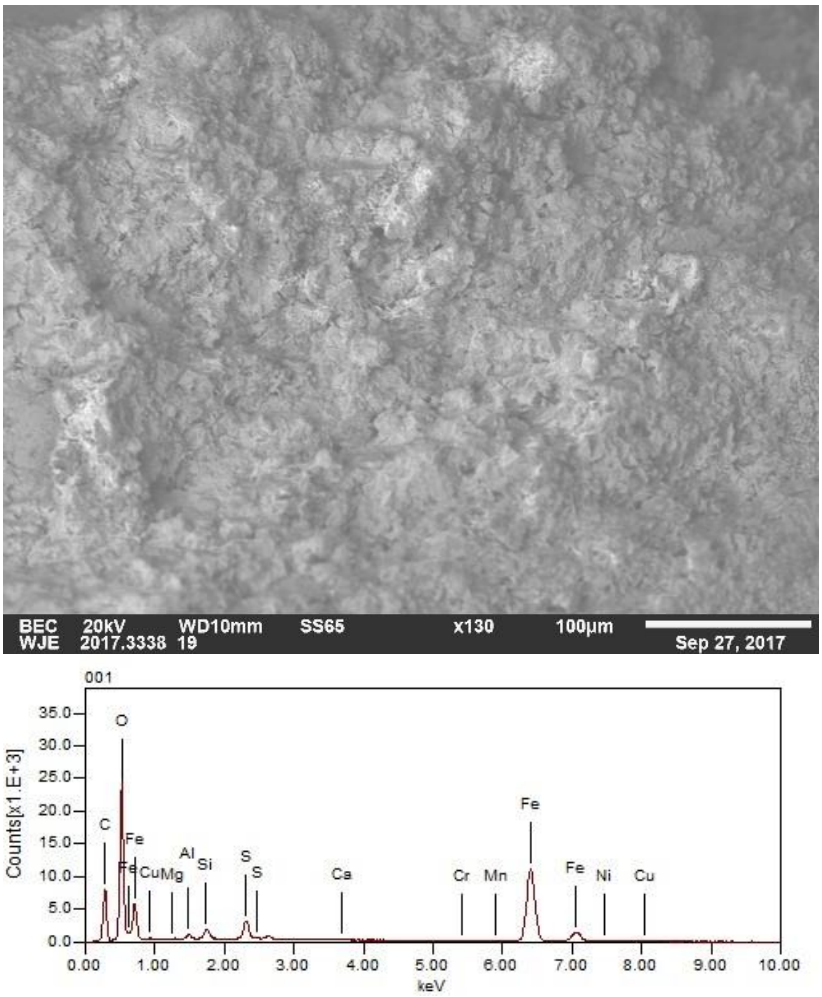

Figure 9. BE micrograph and area EDS spectrum of corrosion product removed from Assembly #19.

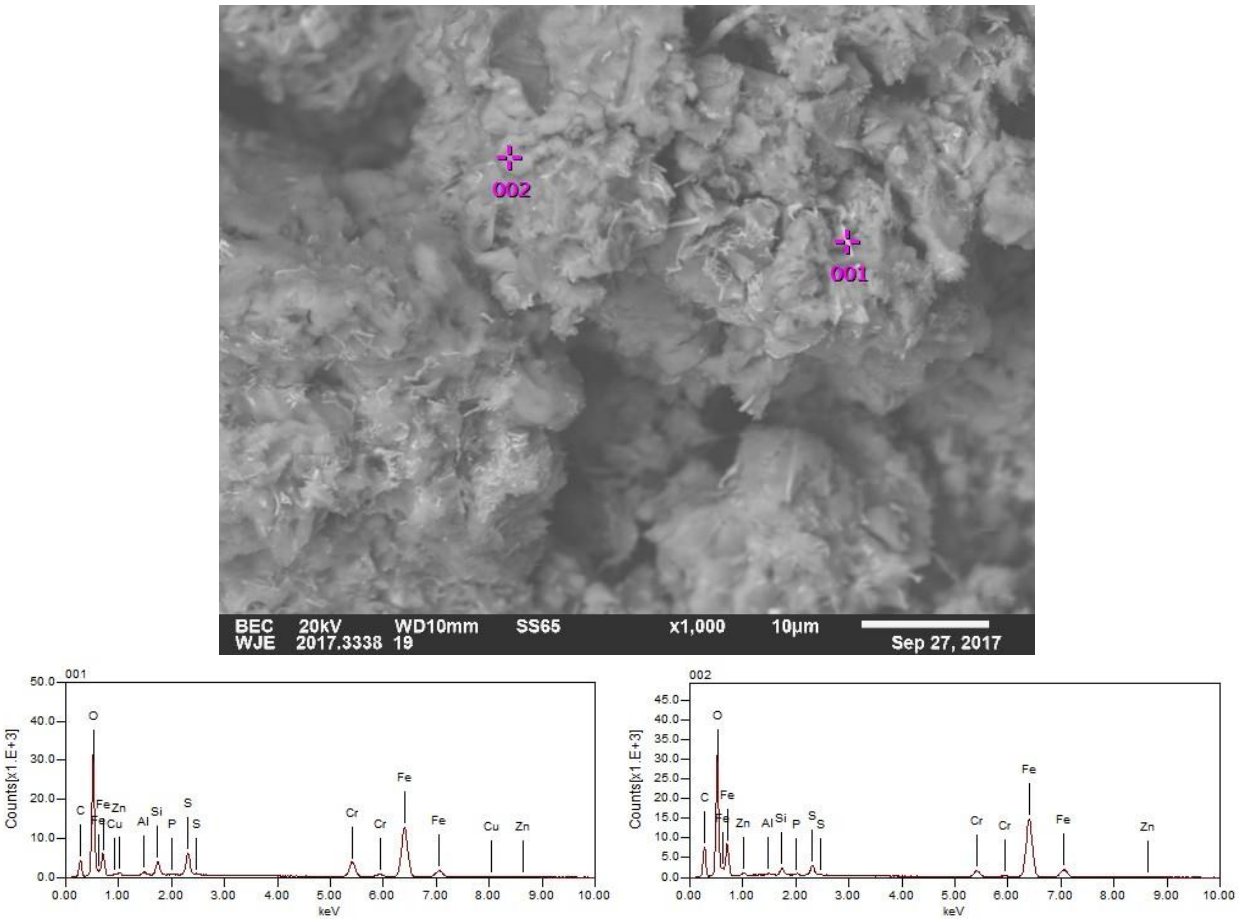

Figure 10. BE micrograph and EDS point spectra of corrosion product removed from Assembly #19. Each EDS spectrum has a number in the upper left corner that corresponds to a point with the same designation in the micrograph.